IEEE Access
Multidisciplinary ⋮ Rapid Review ⋮ Open Access Journal

Received April 30, 2021, accepted May 28, 2021, date of publication June 7, 2021, date of current version June 17, 2021.

Digital Object Identifier 10.1109/ACCESS.2021.3086861

A Variational Bayes Based State-of-Charge Estimation for Lithium-Ion Batteries Without Sensing Current

JING HOU, YAN YANG, AND TIAN GAO

Department of Electronic and Information, Northwestern Polytechnical University, Xi'an 710072, China

Corresponding author: Jing Hou (jhou0825@nwpu.edu.cn)

This work was supported in part by the National Natural Science Foundation of China under Grant 52007156, and in part by the Shaanxi Provincial Key Research and Development Program under Grant 2019GY-003.

ABSTRACT State-of-charge (SOC) estimation of lithium-ion batteries in portable devices without sensing the current is considered in this study. Unlike the traditional approach of separate estimation of the SOC and current, we firstly reformulate the problem as state estimation for the nonlinear system with an unknown input which refers to the current in this study, then a novel variational Bayes-based unscented Kalman filter (VB-UKF) is proposed to simultaneously estimate the SOC and the current input for the nonlinear lithium-ion battery system. Verifications of the SOC estimation performance are made by the experiments under the pulsed-discharge profile and urban dynamometer driving schedule profile. Experimental results show that the proposed VB-UKF algorithm is superior to the unscented recursive three-step filter (URTSF) in terms of convergence rate and estimation accuracy of the SOC and current. And the SOC root mean square errors of VB-UKF are bounded within $\pm 3\%$ after convergence which indicates the feasibility and effectiveness of the proposed method.

INDEX TERMS Battery, state-of-charge, unknown current, unscented Kalman filter, variational Bayes.

I. INTRODUCTION

Recently, lithium-ion batteries have experienced explosive growth for use in a wide range of applications, from portable devices to large-scale high-power energy storage systems [1]. To prevent the abuse usage and make the most of the battery, a battery management system (BMS) must be properly developed. As one of the key tasks of the BMS, accurate estimation of battery state-of-charge (SOC) which quantifies the remaining battery capacity is significant for battery health monitoring [2], charging pattern optimization [3], [4], effective equalization control [5] and fault diagnosis [6]. However, it is impossible to directly measure the SOC because the battery itself is a closed system. Generally, it needs to be estimated from the current and voltage measurements.

Extensive researches have been conducted to improve the SOC estimation accuracy while reducing the computation complexity. The open circuit voltage (OCV) and the ampere-hour (Ah) integration methods are two most conventional direct methods for the SOC estimation. They are simple and easy for implementation. Nonetheless, the precision of the Ah integration method suffers from the erroneous initial SOC value and error accumulation due to noise and drift. The OCV method requires a sufficient resting time to guarantee that the battery terminal voltage measurement is approximately equal to the OCV value, which makes it infeasible for online estimation. To overcome the weaknesses of the direct methods, the model-based estimation approaches have been put forward. Such methods can basically be implemented in two steps.

Firstly, an accurate battery model is established to describe the battery dynamic characteristics. Two representative types of battery models are electrochemical models [8], [9] and equivalent circuit models (ECMs) [10]–[12]. The electrochemical models are highly accurate but with high complexity and heavy computation load in implementation. The ECMs use simple electrical elements, such as resistors and capacitors, to mimic the battery dynamic behaviors. Therefore, it is simple, intuitive and more practical than others. Among the ECMs, the first-order resistor-capacitor (RC) model and the second-order RC model are two most popular models due to their high precision and simple structure.

The associate editor coordinating the review of this manuscript and approving it for publication was Datong Liu.

With the increase of the order of the RC model, the model accuracy will be improved, however, at the cost of additional calculation load. In order to further improve the accuracy of the battery model, reference [13] has considered the hysteresis effect and the current drift of the lithium battery. In addition, the model parameter identification method is crucial for the ECM model reliability and accuracy. One widely used method is the offline parameterized look-up tables which use the stored data to update and calibrate model parameters according to different SOC, temperature and even health status. Hua *et al.* [14] further considered the parameter dependence on the current load and proposed a novel parameter identification method with a parameter switching scheme. Another way of identifying parameters is to use the online methods such as the recursive least squares methods [15], [16] and the dual Kalman type filters [17], which can make real-time corrections of the battery parameters under various operating conditions.

Secondly, the adaptive filters or observers, such as extended Kalman filter (EKF) [17], [18], unscented Kalman filter (UKF) [19], [20], particle filter (PF) [21], sliding mode observer [22] and Luenberger observer [23] are employed to estimate the SOC via the voltage, current, and temperature measurements. Among these algorithms, EKF is the most popular due to its low computational complexity and small need in memory capacity. But, the estimation accuracy of EKF may degrade for highly nonlinear systems on account of the use of the first-order Taylor expansion. By comparison, a third-order Taylor expansion is utilized for the UKF to enhance the SOC estimation accuracy but with heavier computation load. Reference [24] gave the performance evaluation of the EKF, UKF, and PF for lithium battery SOC estimation and showed that the UKF had the best performance in accuracy. Meanwhile, to account for the measurement uncertainty and modeling error, the Sage–Husa estimator is combined with the square root unscented Kalman filter [19] to improve the accuracy of the SOC estimation with adaptive adjustion of the values of the process and measurement covariances. EI Din *et al.* [25] employed a multiple-model EKF (MM-EKF) to estimate SOC under the uncertain measurement noise statistics. In [26], [27], H infinity filters were adopted to deal with the outliers in measurements. Furthermore, a varational Bayes and Huber-based square root cubature Kalman filter [20] for SOC estimation was brought forward to simultaneously handle both modeling errors and outliers in measurements.

However, there exists an issue when applying the adaptive filters to the battery SOC estimation in low-cost portable applications. That is these adaptive filters require the current measurement as an input to estimate the SOC, but the current sensor may not be equipped in portable devices because of the restrictions in cost, volume and power. Therefore, developing a current sensor-less SOC estimation algorithm becomes crucial.

One direct approach is to firstly estimate the current using the battery electrical dynamics and then employ the conventional adaptive filters to obtain the SOC estimation. Putra *et al.* [28] designed a current estimation method based on the Thevenin ECM and Cambron and Cramer [1] employed an unknown input observer to estimate the current. Chun *et al.* [29] extracted the estimated OCV and current information from the filtered terminal voltage, and then calculate the battery SOC using the Ah integration method. However, these methods either utilized a very simple battery model consisting of only a resistor and a capacitor, or adopted a linear relationship between OCV and SOC. These simplifications will bring about precision reduction of the battery model, thus enlarging the current and SOC estimation errors.

A novel treatment is to regard the current as an unknown input and reformulate the SOC estimation problem as optimal filtering problem of nonlinear systems with an unknown input in both the state and measurement equations. Based on this, an unscented recursive three-step filter (URTSF) [30] was proposed in our previous work. It combined the minimum-variance unbiased estimator and the unscented Kalman filter to estimate the state and current input. However, URTSF used the weighted least squares method to estimate the input, which may bring large performance degradation when the measurement errors are largely caused by the measurement noise.

Actually, the Bayesian approach is the most general method for state estimation with some uncertainties. However, it is often computationally complicated. One effective approximation method is the variational Bayesian (VB) inference method, which approximates the joint posterior with a product of tractable marginal posteriors by virtue of the variational ideas [31]. Some researchers have developed this method for state estimation with unknown statistical properties of the measurement noise [32], [33]. In [34], the VB method was proposed for state estimation of linear systems with unknown inputs. In this study, the VB approach was used to approximate the joint posterior of the state and the input, and then a recursive filtering algorithm combined with the UKF for nonlinear systems was derived. It can achieve the simultaneous estimation of the SOC and current, and has a better SOC estimation performance than the URTSF under different operating conditions.

The main contribution of this study is: (1) The SOC estimation problem without current measurement is novelly reformulated as the optimal filtering problem of nonlinear system with an unknown input, and the VB method combined with the UKF is proposed to solve this problem; (2) Compared with URTSF which estimates the current using weighted least squares, the proposed algorithm realizes simultaneous estimation of the SOC and current for the nonlinear lithium-ion battery system; (3) Pulsed-discharge test and urban dynamometer driving schedule (UDDS) test are conducted to verify the SOC estimation performance. Experiment results show that the proposed VB-UKF outperforms URTSF in terms of convergence rate and SOC estimation accuracy.

The remainder of this paper is arranged as follows. The battery is modeled in Section II. In Section III, the VB-based UKF algorithm for joint estimation of SOC and current is presented. Section IV provides the experimental results and analysis of the proposed algorithm. Finally, Section V reports the conclusions.

II. BATTERY MODEL AND PARAMETER IDENTIFICATION

A. BATTERY MODEL

It is well known that an accurate battery model is critical for the performance of SOC and parameters estimation. Therefore, various battery models have been raised, among which the first-order RC and second-order RC ECM models are the two most commonly used battery models. Reference [10] pointed out that the first-order RC has excellent reliability, while the second-order RC has better accuracy of ECM, and these two have almost the same SOC estimation accuracy, but the second-order RC is much more complicated than the first-order RC. Therefore, considering the computation capacity in portable applications, we make a trade-off between model accuracy, reliability and computation cost, and select the first-order RC model shown in Fig. 1 as the battery model.

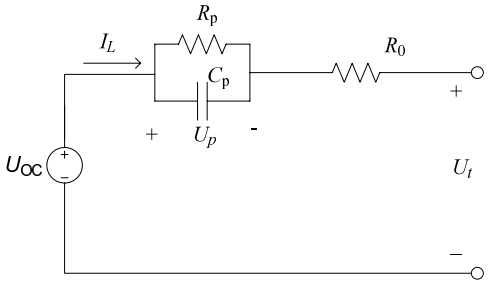

FIGURE 1. First-order RC model of the battery.

In the figure, U_{oc} denotes the OCV, U_t refers to the battery terminal voltage, I_L stands for the load current, R_0 indicates the ohmic internal resistance. A parallel RC network composed by the polarization resistance R_p and polarization capacitance C_p is used to capture the battery relaxation effect, U_p describes the polarization voltage. Based on this model and the Kirchhoff's law, the battery electrical behavior can be written as follows:

$$U_t = U_{oc} - U_p - I_L R_0, \tag{1}$$

$$\dot{U}_p = \frac{I_L}{C_p} - \frac{U_p}{R_p C_p}, \tag{2}$$

Generally, the SOC is calculated using the Ah integral method as:

$$SOC_t = SOC_{t_0} - \frac{1}{Q_{rate}} \int_{t_0}^{t} \eta_c I_{L,t} dt, \tag{3}$$

where, Q_{rate} and η_c represent the rated capacity and Coulomb efficiency respectively.

Discretizing (1)-(3), the discrete-time state-space equations are expressed as:

$$x_{k+1} = f(x_k, I_{L,k}) + w_k, \tag{4}$$

$$y_k = h(x_k, I_{L,k}) + v_k, \tag{5}$$

where, $x = [SOC, U_p]^T$ is the state vector, w_k and v_k represent the Gaussian process noise with covariance Q_k and measurement noise with variance R_k, respectively. They are both zero-mean noises, without any shifts. That is, we do not consider the outliers and the shift noise in this study. $f(\cdot)$ and $h(\cdot)$ represent the state transition function and measurement function, respectively, expressed as

$$f(\cdot) = \begin{bmatrix} 1 & 0 \\ 0 & e^{-\frac{\Delta t}{\tau_p}} \end{bmatrix} \begin{bmatrix} SOC_k \\ U_{p,k} \end{bmatrix} + \begin{bmatrix} -\frac{\eta \Delta t}{Q_{rate}} \\ R_p(1 - e^{-\frac{\Delta t}{\tau_p}}) \end{bmatrix} I_{L,k}, \tag{6}$$

$$h(\cdot) = U_{OC}(SOC_k) - U_{p,k} - I_{L,k} R_0, \tag{7}$$

where, Δt is the sampling period, $\tau_p = R_p C_p$. $U_{OC}(SOC_k)$ describes the OCV-SOC nonlinear relationship.

B. PARAMETER IDENTIFICATION

The first-order RC battery model contains three parameters: R_0, R_p, C_p and the OCV-SOC relationship. To identify these parameters, the following test procedure was designed:

1) EXPERIMENTAL SETUP

The experimental battery is a SAMSUNG ICR18650 lithium-ion battery with a rated capacity and rated voltage of 2600 mAh and 3.63 V, respectively. The experimental platform consists of a battery test system (NEWARE BTS4000) and a personal computer for controlling the test system and collecting the test data.

2) OCV-SOC CURVES DETERMINATION

A pulsed-discharge test was implemented to determine the OCV-SOC curve and the model parameters. (a). First, fully charge the battery to 100% SOC and stand for 1 hour. Then the OCV value can be obtained by measuring the terminal voltage. (b). Discharge the battery for 10 seconds with a $1/3C$ constant current rate and measure the terminal voltage after resting for 30 minutes. (c). Continue to discharge until 5% of the nominal capacity is consumed, and rest for 1 hour, then measure the OCV. (d). Repeat steps (b)-(c) till the lower cut-off voltage is reached.

After the above pulsed-discharge test, the OCV measurement corresponding to each SOC point were collected. Based on the tested data, the OCV-SOC relationship was characterized using a seventh-order polynomial model in Equation (8), and the measured voltage and fitted curve are presented in Fig. 2. It is clear that R-square is close to 1 which indicates good curve fitting [35]. This result shows that the measurement data were well fitted to the seventh-order

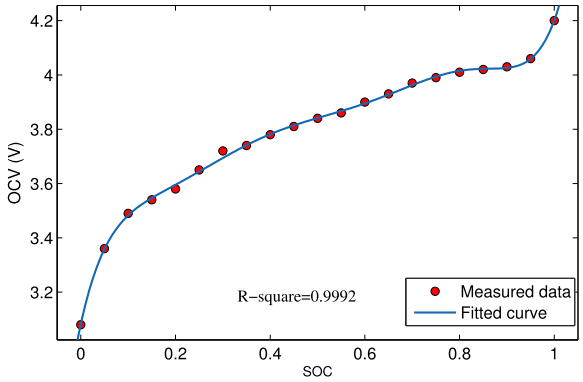

FIGURE 2. The OCV-SOC relationship curve.

polynomial model.

$$U_{oc}(SOC) = 3.082 + 8.008 \times SOC - 61.8 \times SOC^2 + 278.5 \times SOC^3 - 691.2 \times SOC^4 + 945.2 \times SOC^5 - 666.5 \times SOC^6 + 189 \times SOC^7. \quad (8)$$

3) BATTERY PARAMETERS DETERMINATION

From the terminal voltage response to the pulsed current in step (b), as shown in Fig. 3, the battery model parameters can be identified. At the instant the discharge current is loaded, the terminal voltage is rapidly reduced from U_1 to U_2. This is mainly attributed to the ohmic internal resistance. With the continuous discharge, the voltage drops slowly from U_2 to U_3 as a result of a polarization reaction by R_p and C_p. When the discharge stops, the voltage rises quickly from U_3 to U_4. After standing for a period of time, the battery voltage tends to be stable.

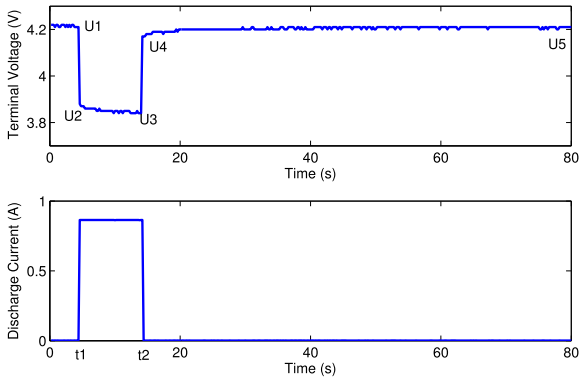

FIGURE 3. The terminal voltage and current curve of one single pulse discharge cycle.

From the above analysis, the ohmic internal resistance can be obtained as:

$$R_0 = \frac{U_1 - U_2}{I_L}. \quad (9)$$

The voltage variations from U_4 to U_5 can be regarded as the zero-input response of the RC circuit. Thus, the terminal voltage response can be written as

$$U_t(t) = U_{oc} - U_p(0)\exp(-t/\tau_p), \quad (10)$$

where, U_{oc} is the OCV, $U_p(0)$ is the initial polarization voltage. $U_p(0)$ and τ_p can be obtained using the least squares algorithm.

During the discharge process from t_1 to t_2, the terminal voltage decreases slowly from U_2 to U_3. This stage can be regarded as the zero-state response of the RC circuit. Thus, the voltage response can be written as:

$$U_t(t) = U_{oc} - R_p I_L(1 - \exp(-t/\tau_p)) - R_0 I_L, \quad (11)$$

R_p can be obtained using the least squares algorithm. C_p can then be calculated. The identified battery model parameters R_0, R_p, C_p are shown in Table 1.

Using the cftool toolbox in Matlab, the fitting functions can be obtained as follows:

$$R_0 = -12.72 + 16.1SOC + 34.68e^{-0.7576SOC} \quad (12)$$

$$R_p = -24.54 + 101.2SOC + 42.31SOC^2 - 116.2 \times SOC^3 - 101.8SOC^4 + 123.6SOC^5 + 58.47e^{-4.107SOC} \quad (13)$$

$$C_p = 1371 - 1.193e^4SOC + 7.774e^4SOC^2 - 2.027e^5 \times SOC^3 + 2.259e^5SOC^4 - 8.978SOC^5 \quad (14)$$

Based on these fitting functions, the battery parameters can be calculated at each SOC point. But it should be noted that these fitting functions are obtained based on the experiment data from a brand new battery under the room temperature. With the variations of the temperatures and the health status, the battery parameters will greatly change, which may no more fit the above functions. However, this weakness can be surmounted by establishing the fitting functions under different temperatures and states of health, as part of future work.

C. MODEL VALIDATION

The battery model was validated through comparing the measured and estimated terminal voltages under the pulsed-discharge and UDDS tests, as shown in Fig. 4. The maximum modeling error is less than 10 mV in the pulsed-discharge test, while an error of less than 3 mV is observed in the UDDS test. In both two tests, the maximum errors appear during periods of transient current, but under the steady-state current condition, the modeling errors tend to be 0 mV. These findings indicate that this ECM model is sufficient to simulate the electrical behaviour of the battery.

III. SOC ESTIMATION ALGORITHM WITH UNKNOWN CURRENT INPUT USING VARIATIONAL BAYESIAN METHOD

As we know, Bayesian approach is a general method for optimal filtering of systems with unknown parameters. However, it is usually difficult to obtain the analytical solution

TABLE 1. The identified parameters of the battery model.

SOC	1	0.95	0.9	0.85	0.8	0.75	0.7	0.65	0.6	0.55
$R_0(m\Omega)$	19.57	19.48	19.59	19.25	19.03	19.11	18.57	18.62	18.58	19.26
$R_p(m\Omega)$	26.64	23.32	22.39	23.65	24.34	26.58	28.43	27.84	28.85	27.11
$C_p(F)$	619.40	835.54	1104.92	1002.35	945.61	832.63	637.55	722.56	646.45	603.87
SOC	0.5	0.45	0.4	0.35	0.3	0.25	0.2	0.15	0.1	0.05
$R_0(m\Omega)$	19.58	19.37	19.09	19.42	20.04	20.11	20.09	20.54	21.09	21.48
$R_p(m\Omega)$	22.45	25.63	28.70	24.23	21.76	22.09	21.02	20.91	28.46	26.53
$C_p(F)$	999.19	1012.58	977.01	887.31	803.77	756.69	876.77	842.33	788.73	905.41

due to high complexity. Recently, the variational Bayes (VB) method [34], [36] has been proposed to approximate the joint posterior at a low computational cost. It is a useful tool to solve the problem of state estimation with unknown input.

First, we rewrite the state and measurement equations for SOC estimation as:

$$\begin{aligned} x_{k+1} &= f(x_k, d_k) + w_k, \\ y_k &= h^*(x_k) + G_k d_k + v_k, \end{aligned} \tag{15}$$

where $x_k \in R^n$ denotes the system state; $y_k \in R^p$ stands for the measurement vector. $d_k \in R^m$ refers to the current, it is an unknown input vector. w_k and v_k are process and measurement noises which are Gaussian distributed with zero mean and covariances Q_k and R_k, respectively. $h^*(x_k) = U_{oc}(SOC_k) - U_{p,k}$, $G_k = -R_0$.

The basic idea of VB approach is to approximate the joint posterior of x_k and d_k with the product of two tractable marginal posteriors as:

$$p(x_k, d_k|y_{1:k}) \approx Q(x_k, d_k) = Q_x(x_k)Q_d(d_k). \tag{16}$$

By minimizing the Kullback-Leibler (KL) divergence from the exact posterior $p(x_k, d_k|y_{1:k})$ to the approximating posterior $Q(x_k, d_k)$, $Q_x(x_k)$ and $Q_d(d_k)$ can be obtained as

$$Q_x(x_k) \propto \exp\left(\int \log p(y_k, x_k, d_k|y_{1:k-1})Q_d(d_k)\mathrm{d}d_k\right), \tag{17}$$

$$Q_d(d_k) \propto \exp\left(\int \log p(y_k, x_k, d_k|y_{1:k-1})Q_x(x_k)\mathrm{d}x_k\right). \tag{18}$$

For the above system (15), the likelihood of the measurement at time k is

$$p(y_k|x_k, d_k) = N(y_k; h^*(x_k) + G_k d_k, R_k), \tag{19}$$

and we assume d_k has Gaussian prior density by conjugacy, that is

$$p(d_k|y_{1:k-1}) = N(d_k; \hat{\mu}_{k|k-1}, \Sigma_{k|k-1}), \tag{20}$$

and the prediction density of x_k is

$$p(x_k|y_{1:k-1}) = N(x_k; \hat{x}_{k|k-1}, P_{k|k-1}). \tag{21}$$

Then, the logarithm of (17) and (18) can be expanded as

$$\begin{aligned} log Q_x(x_k) &= \int \log p(y_k, x_k, d_k|y_{1:k-1})Q_d(d_k)\mathrm{d}d_k \\ &= \int \log p(y_k|x_k, d_k)p(x_k|y_{1:k-1}) \\ &\quad \times p(d_k|y_{1:k-1})Q_d(d_k)\mathrm{d}d_k \\ &= -\frac{1}{2}\langle (y_k - h^*(x_k) - G_k d_k)^T R_k^{-1}(y_k \\ &\quad - h^*(x_k) - G_k d_k)\rangle_{d_k} - \frac{1}{2}(x_k - \hat{x}_{k|k-1})^T \\ &\quad \times P_{k|k-1}^{-1}(x_k - \hat{x}_{k|k-1}) + const, \end{aligned} \tag{22}$$

$$\begin{aligned} log Q_d(d_k) &= \int \log p(y_k, x_k, d_k|y_{1:k-1})Q_x(x_k)\mathrm{d}x_k \\ &= \int \log p(y_k|x_k, d_k)p(d_k|y_{1:k-1}) \\ &\quad \times p(x_k|y_{1:k-1})Q_x(x_k)\mathrm{d}x_k \\ &= -\frac{1}{2}\langle (y_k - h^*(x_k) - G_k d_k)^T R_k^{-1}(y_k \\ &\quad - h^*(x_k) - G_k d_k)\rangle_{x_k} - \frac{1}{2}(d_k - \hat{\mu}_{k|k-1})^T \\ &\quad \times \Sigma_{k|k-1}^{-1}(d_k - \hat{\mu}_{k|k-1}) + const, \end{aligned} \tag{23}$$

where $\langle\cdot\rangle_{d_k}$ and $\langle\cdot\rangle_{x_k}$ denote the expectations with respect to $Q_d(d_k)$ and $Q_x(x_k)$, respectively.

If the VB marginal distribution is $Q_d(d_k) = N(d_k; \hat{\mu}_{k|k}, \Sigma_{k|k})$, where, $\hat{\mu}_{k|k}$ stands for the mean value of the current estimate at time k, $\Sigma_{k|k}$ is a variance which reflects the uncertainty range of the estimate. Using the formulas of the product of two Gaussian probability density functions, we can derive

$$\begin{aligned} \Sigma_{k|k}^{-1} &= \Sigma_{k|k-1}^{-1} + G_k^T R_k^{-1} G_k, \\ \Sigma_{k|k}^{-1}\hat{\mu}_{k|k} &= \Sigma_{k|k-1}^{-1}\hat{\mu}_{k|k-1} + G_k^T R_k^{-1}(y_k - h^*(\hat{x}_{k|k})). \end{aligned} \tag{24}$$

Similarly, if $Q_x(x_k) = N(x_k; \hat{x}_{k|k}, P_{k|k})$, after the linearization processing of $h^*(\cdot)$, we can derive

$$\begin{aligned} P_{k|k}^{-1} &= P_{k|k-1}^{-1} + H_k^T R_k^{-1} H_k, \\ P_{k|k}^{-1}\hat{x}_{k|k} &= P_{k|k-1}^{-1}\hat{x}_{k|k-1} + H_k^T R_k^{-1}(y_k - G_k\hat{\mu}_{k|k}), \end{aligned} \tag{25}$$

where, H_k is the Jacobian matrix of $h^*(\cdot)$. $\hat{x}_{k|k}$ denotes the SOC estimate at time k, $P_{k|k}$ is the covariance which quantifies the uncertainty of the SOC estimate.

We note that (24)-(25) are coupled. If $\hat{\mu}_{k|k}$ is known, (25) is actually the standard Kalman filter. It is the same for (24) if $\hat{x}_{k|k}$ is known. That is, the VB adaptive filter for the systems with unknown input can be implemented within the Kalman filter framework. Nevertheless, in view of the nonlinear measurement equation and the coupling of

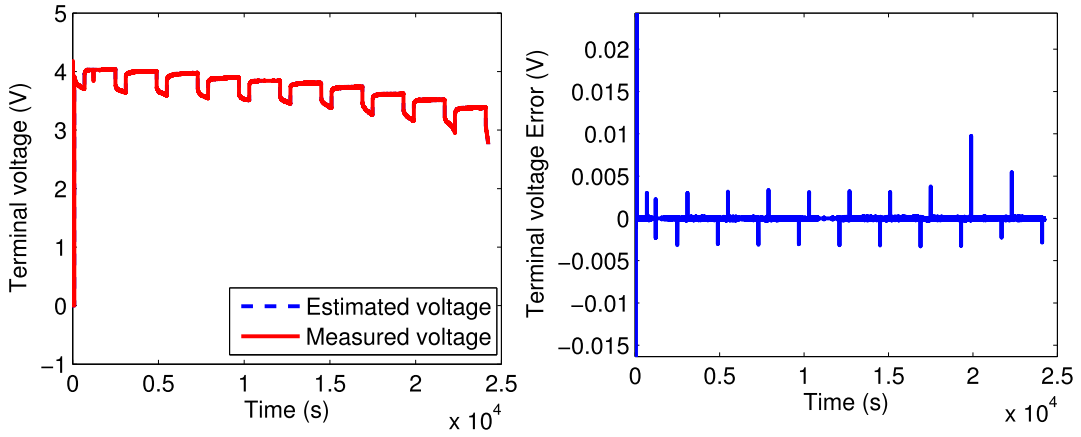

(a) Pulsed-discharge test

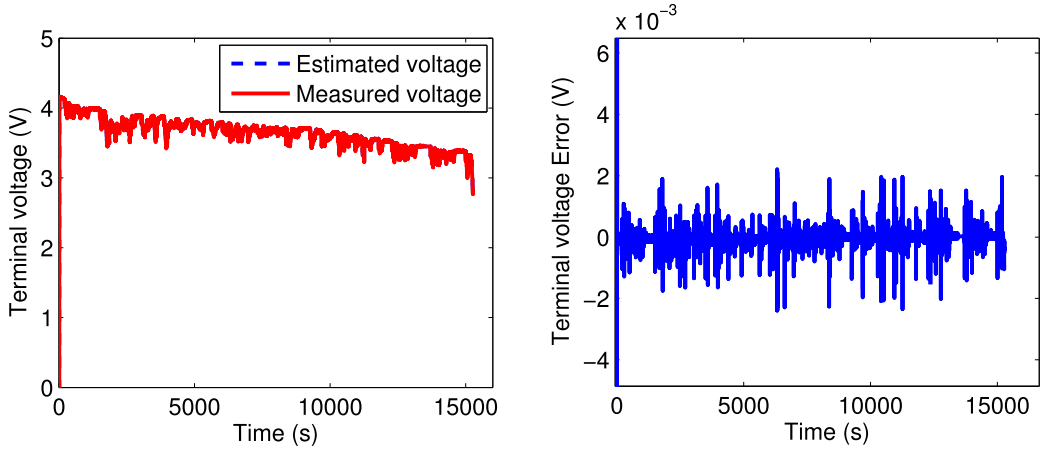

(b) UDDS test

FIGURE 4. Estimated and measured terminal voltages under different tests.

the system state and input, a nonlinear filter implementation is requisite. As pointed out in [24], UKF has much better performance than EKF in terms of accuracy and convergence rate at the cost of more computation time than EKF. Considering the used simple first-order RC ECM, the estimated state is only 2 dimensional, thus the use of UKF will impose not so much computation burden but provide a significant SOC performance boost. Therefore, we choose to iteratively utilize the UKF to estimate the system state and the standard KF to estimate the input. The flowchart of the proposed algorithm VB-UKF is shown in Fig. 5. The filtering process is summarized as follows.

Step 1. Initialize the state and input estimates and their covariances: $\hat{x}_{0|0}$, $P_{0|0}$, Q_0, $\hat{\mu}_{0|0}$, $\Sigma_{0|0}$.

Step 2. Prediction ($k = 1, 2, 3, \ldots$).

Step 2.1 Calculate sigma points and weights:

$$\begin{cases} \xi_{k-1}^{0} = \hat{x}_{k-1|k-1} \\ \xi_{k-1}^{i} = \hat{x}_{k-1|k-1} + \left(\sqrt{(n_x + \lambda_x) P_{k-1|k-1}}\right)_i \\ \xi_{k-1}^{i+n_x} = \hat{x}_{k-1|k-1} - \left(\sqrt{(n_x + \lambda_x) P_{k-1|k-1}}\right)_i \\ \qquad i = 1, \cdots, n_x, \end{cases} \tag{26}$$

$$\begin{cases} W_0^m = \lambda_x/(n_x + \lambda_x) \\ W_0^c = \lambda_x/(n_x + \lambda_x) + (1 - \alpha_x^2 + \beta_x) \\ W_i^m = W_i^c = 1/[2(n_x + \lambda_x)], \quad i = 1, \cdots, 2n_x, \end{cases} \tag{27}$$

where, W_i^m and W_i^c denote the weighted factors of the mean and covariance, respectively; n_x is the dimension of the state vector. λ_x is a composite coefficient and defined by $\lambda_x = \alpha_x^2(n_x + \kappa_x) - n_x$. Here we assume $0 < \alpha_x < 1$, $\kappa_x = 0$, $\beta_x = 2$.

Step 2.2 Compute the predicted state value and its covariance:

$$\xi_{k|k-1}^{i} = f(\xi_{k-1}^{i}, \hat{\mu}_{k-1|k-1}), \tag{28}$$

$$\hat{x}_{k|k-1} = \sum_{i=0}^{2n_x} W_i^m \xi_{k|k-1}^{i}, \tag{29}$$

$$P_{k|k-1} = \sum_{i=0}^{2n_x} W_i^c (\xi_{k|k-1}^{i} - \hat{x}_{k|k-1})(\xi_{k|k-1}^{i} - \hat{x}_{k|k-1})^T + Q_k. \tag{30}$$

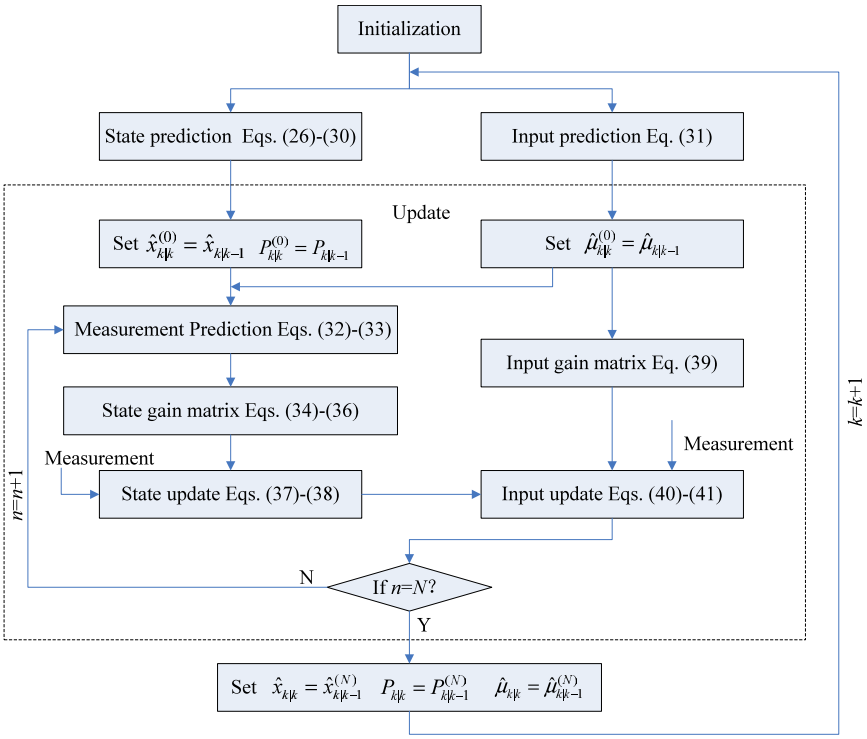

FIGURE 5. Flowchart of the proposed algorithm VB-UKF.

Step 2.3 Compute the predicted input estimate and its covariance:

$$\hat{\mu}_{k|k-1} = \rho\hat{\mu}_{k-1|k-1}, \quad \Sigma_{k|k-1} = \rho\Sigma_{k-1|k-1}, \tag{31}$$

where, ρ is a scale factor with values satisfying $0 < \rho < 1$. The value $\rho = 1$ corresponds to stationary current and variance. The current fluctuates faster as the value of ρ decreases.

Step 3. Update: first set: $\hat{x}_{k|k}^{(0)} = \hat{x}_{k|k-1}$, $P_{k|k}^{(0)} = P_{k|k-1}$, $\hat{\mu}_{k|k}^{(0)} = \hat{\mu}_{k|k-1}$, and then for $n = 0 : N-1$, iterate the following update steps, where N refers to the number of iterations, which depends on the accuracy requirement and usually takes on values of 1-10.

Step 3.1 Calculate the predicted measurement:

$$y_{k|k-1}^{i,(n+1)} = h^*(\xi_{k|k-1}^i) + G_k\hat{\mu}_{k|k}^{(n)}, \tag{32}$$

$$\hat{y}_{k|k-1}^{(n+1)} = \sum_{i=0}^{2n_x} W_i^m y_{k|k-1}^{i,(n+1)}. \tag{33}$$

Step 3.2 Calculate the innovation covariance and the covariance of the innovation and the state:

$$P_{yy,k}^{(n+1)} = \sum_{i=0}^{2n_x} W_i^c (y_{k|k-1}^{i,(n+1)} - \hat{y}_{k|k-1}^{(n+1)})(y_{k|k-1}^{i,(n+1)} - \hat{y}_{k|k-1}^{(n+1)})^T + R_k, \tag{34}$$

$$P_{xy,k}^{(n+1)} = \sum_{i=0}^{2n_x} W_i^c (\xi_{k|k-1}^i - \hat{x}_{k|k-1})(y_{k|k-1}^{i,(n+1)} - \hat{y}_{k|k-1}^{(n+1)})^T. \tag{35}$$

Step 3.3 Calculate the state estimate and its covariance:

$$K_x^{(n+1)} = P_{xy,k}^{(n+1)}(P_{yy,k}^{(n+1)})^{-1}, \tag{36}$$

$$\hat{x}_{k|k}^{(n+1)} = \hat{x}_{k|k-1} + K_x^{(n+1)}(y_k - \hat{y}_{k|k-1}^{(n+1)}), \tag{37}$$

$$P_{k|k}^{(n+1)} = P_{k|k-1} - K_x^{(n+1)} P_{yy,k}^{(n+1)}(K_x^{(n+1)})^T. \tag{38}$$

Step 3.4 Calculate the input estimate and its covariance using KF:

$$K_d = \Sigma_{k|k-1}G_k^T(G_k\Sigma_{k|k-1}G_k^T + R_k)^{-1}, \tag{39}$$

$$\Sigma_{k|k} = \Sigma_{k|k-1} - K_d G_k \Sigma_{k|k-1}, \tag{40}$$

$$\hat{\mu}_{k|k}^{(n+1)} = \hat{\mu}_{k|k-1} + K_d[y_k - h^*(\hat{x}_{k|k}^{(n+1)}) - G_k\hat{\mu}_{k|k-1}]. \tag{41}$$

Step 3.5. Until $n = N-1$, set $\hat{x}_{k|k} = \hat{x}_{k|k}^{(N)}$, $P_{k|k} = P_{k|k}^{(N)}$, $\hat{\mu}_{k|k} = \hat{\mu}_{k|k}^{(N)}$ and end for.

Step 4. $k \to k+1$, return to Step 2 for the next time.

IV. EXPERIMENT AND ANALYSIS

Verification of the proposed VB-UKF method was conducted by a pulsed-discharge test and UDDS test on the lithium-ion battery. UDDS, also known as FTP72, simulates the urban road driving conditions of vehicles, which can be used to test the performance of the proposed algorithm under dynamic operating conditions. Note that the cell current was scaled down according to the cell tolerance in this study. The current profiles of both tests are shown in Fig. 6. In each test, the sampling periods of battery current and voltage were both

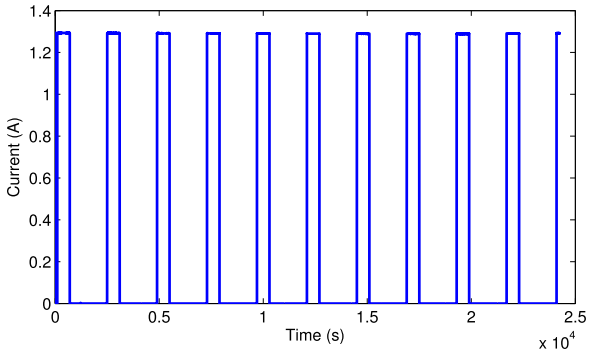

(a) Pulsed-discharge test

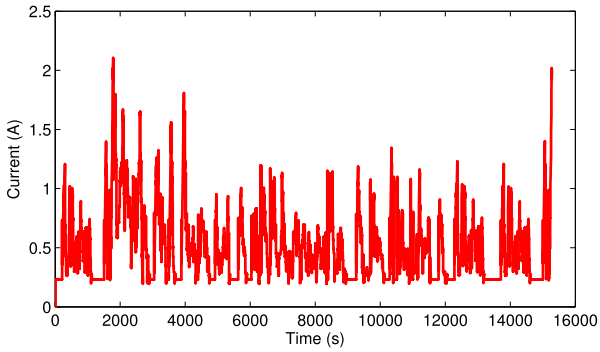

(b) UDDS test

FIGURE 6. Measured current under the pulsed-discharge and UDDS tests.

1 s and the real initial SOC value was 1.0. The real SOC was obtained by the Ah integration method with the actual measured current. Evaluation of the proposed algorithm was conducted by comparison with URTSF algorithm in terms of convergence time and SOC estimation accuracy. The mean absolute error (MAE) and the root mean square error (RMSE) after convergence were employed to indicate the SOC estimation accuracy. The standard deviations of the SOC and current estimates of VB-UKF are used to quantify the estimation uncertainty caused by the difference between the real state and the state estimation [37]. The convergence time refers to the time after which most of the SOC estimation errors are within the bound of $\pm 5\%$.

A. EVALUATION IN PULSED-DISCHARGE TEST

The battery was discharged for 10 minutes at a rate of 0.5C and rested for 30 minutes in one cycle of the pulsed-discharge test. The total discharge process contains 10 cycles. Three different initial SOC values, 1.0, 0.8 and 0.6 are assumed to compare the convergence rate of these algorithms. The measurement noise variance is 0.001 and the process noise covariances are set as $\mathtt{diag}(10^{-6}, 0.1)$ for $SOC = 1.0$ and $\mathtt{diag}(10^{-4}, 0.1)$ for $SOC = 0.8$ and $SOC = 0.6$. We assume a diffuse prior for current as $d_0 \sim N(0, 0.01)$ in the proposed algorithm.

Fig. 7 shows the current estimation results under the pulsed-discharge test. Clearly, VB-UKF has more accurate current estimate than URTSF especially at the end of the discharge. When $SOC_0 = 1$, the maximum absolute errors after convergence are $1.02A$ and $1.45A$, and the MAEs are $0.18A$ and $0.25A$ for VB-UKF and URTSF, respectively. Meanwhile, it can be seen that there is a large error when an abrupt change occurs on the current. But the estimation error quickly decreases during the resting time. It implies that the rest period is helpful for improving the current estimation accuracy. Besides, little differences are observed for the current estimation errors and the uncertainty regions under different initial SOC values. It reveals that the initial SOC errors have no significant impact on the current estimation accuracy for both VB-UKF and URTSF.

The SOC estimation results under different initial SOC estimation errors are presented in Fig. 8. The statistical error analysis and the convergence time of these algorithms are summarized in Table 2. Obviously, the proposed VB-UKF exhibited best performance in terms of convergence rate and SOC estimation accuracy. As can be seen from the figure, the degree of uncertainty increases slightly with the increase of the initial SOC error. When the initial SOC values are 1.0 and 0.8, significant superiority of VB-UKF is observed. The MAE and RMSE of VB-UKF are at least 30% smaller than URTSF, and the convergence times are only about $1/7$ and $2/5$ of URTSF at $SOC_0 = 1$ and $SOC_0 = 0.8$, respectively. But when $SOC_0 = 0.6$, the convergence time of VB-UKF increases dramatically and reaches to 11058s, which is comparable to the convergence time of URTSF, 10349s. This is probably because that severe initial SOC errors need a longer period of time to correct without the actual current measurement. But once convergence, the MAE and RMSE of both algorithms are smaller than 3%, which basically satisfy the requirement of BMS.

TABLE 2. Error analysis and convergence time with different SOC_0 in pulsed-discharge test.

SOC_0	Algorithm	MAE	RMSE	Convergence time (s)
1.0	VB-UKF	1.52%	1.93%	401
	URTSF	2.65%	2.91%	2735
0.8	VB-UKF	1.67%	2.00%	2954
	URTSF	2.28%	2.69%	7542
0.6	VB-UKF	2.16%	2.73%	11058
	URTSF	2.58%	2.92%	10349

In addition, the SOC and current estimation results are compared. When $SOC_0 = 1$, URTSF has larger current estimation errors than VB-UKF at the beginning of the discharge, and correspondingly larger SOC estimation errors are observed in Fig. 8(a) for URTSF. It shows that the precision of the current estimation has an influence on the SOC estimation accuracy. But when $SOC_0 = 0.8$ and $SOC_0 = 0.6$, the SOC estimation errors in the beginning are mainly caused by the initial SOC error. Once convergence, the current estimation error becomes a more important influence factor for the SOC estimation accuracy.

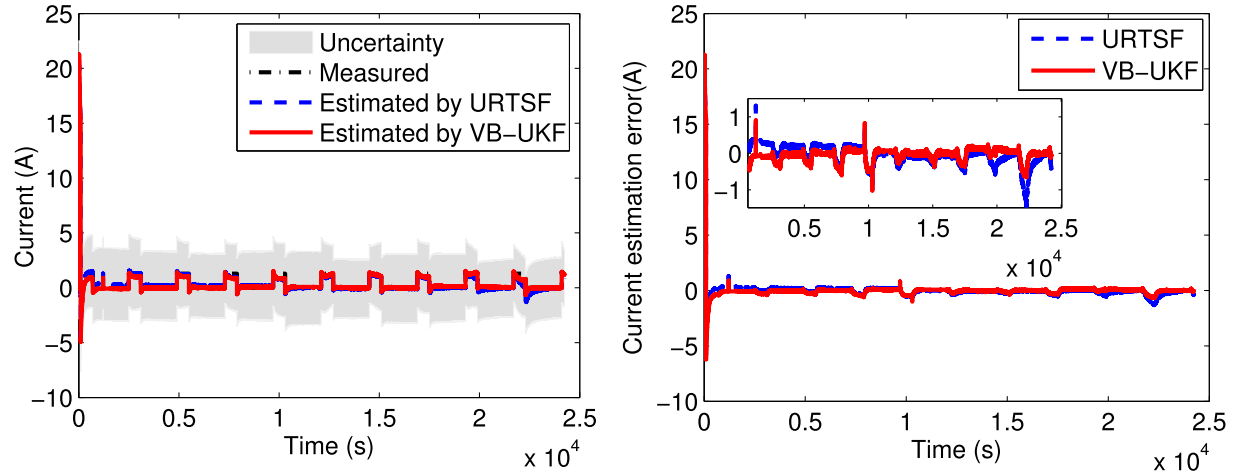

(a) $SOC_0 = 1.0$

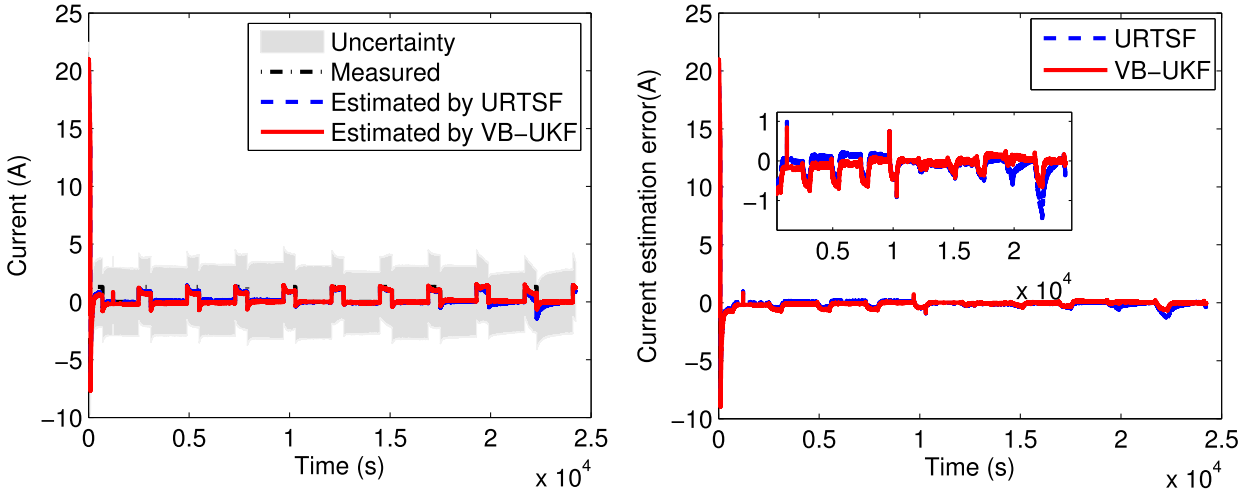

(b) $SOC_0 = 0.8$

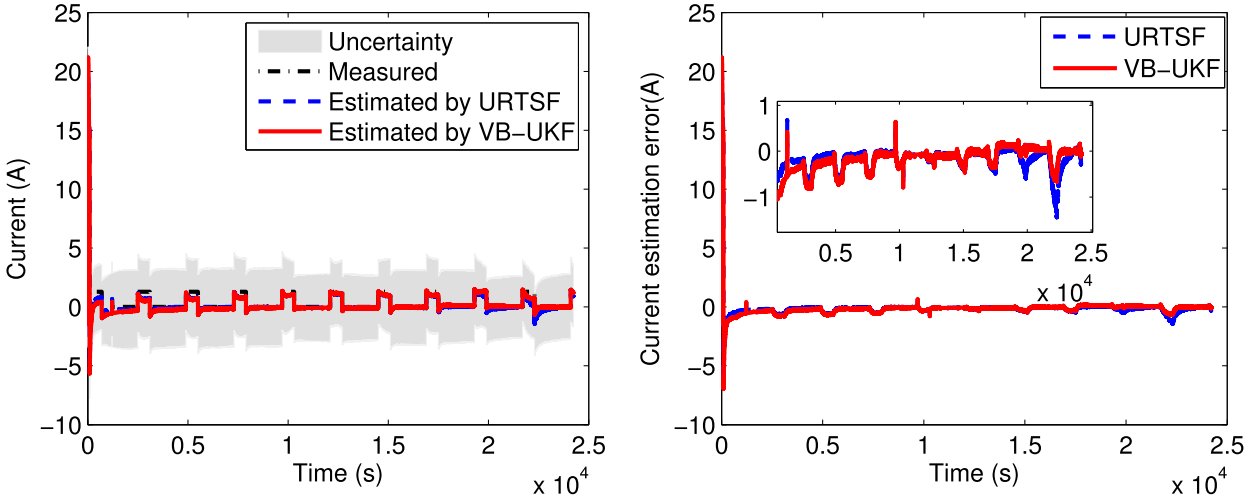

(c) $SOC_0 = 0.6$

FIGURE 7. Current estimation results in pulsed-discharge test with different initial values (SOC_0).

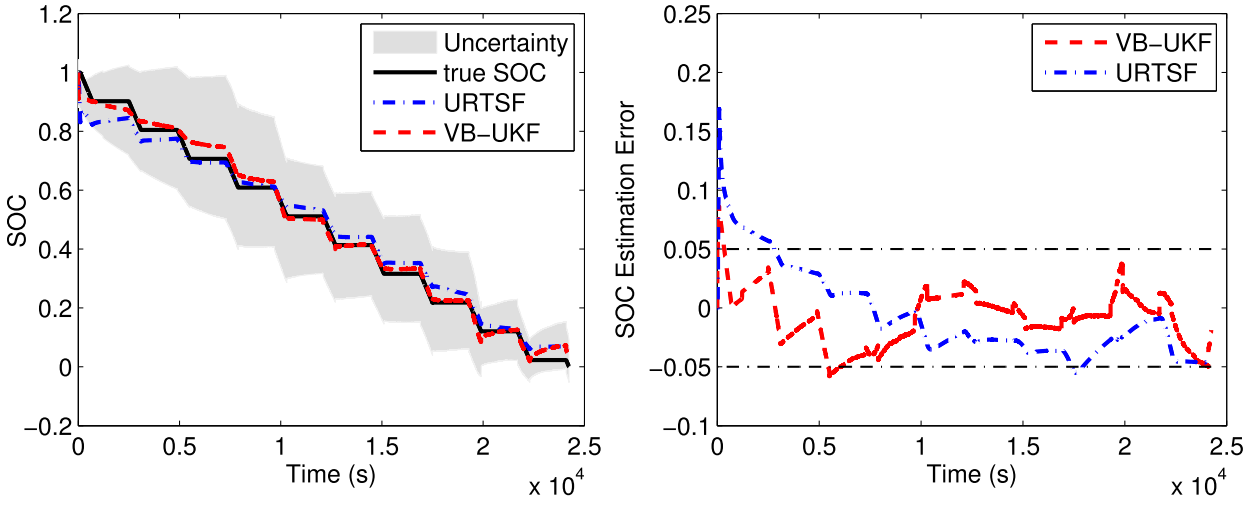

(a) $SOC_0 = 1.0$

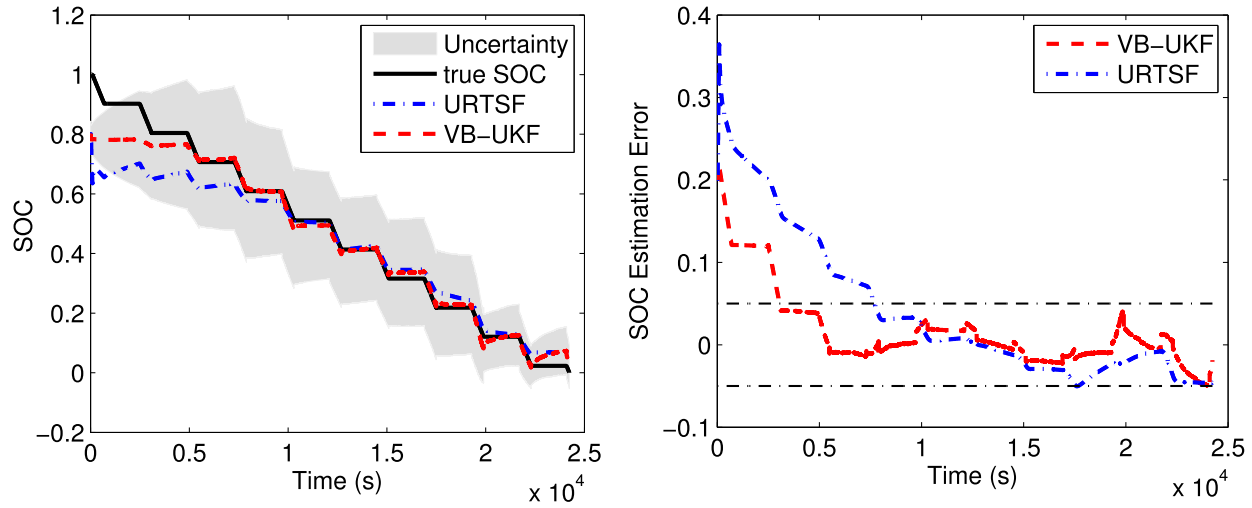

(b) $SOC_0 = 0.8$

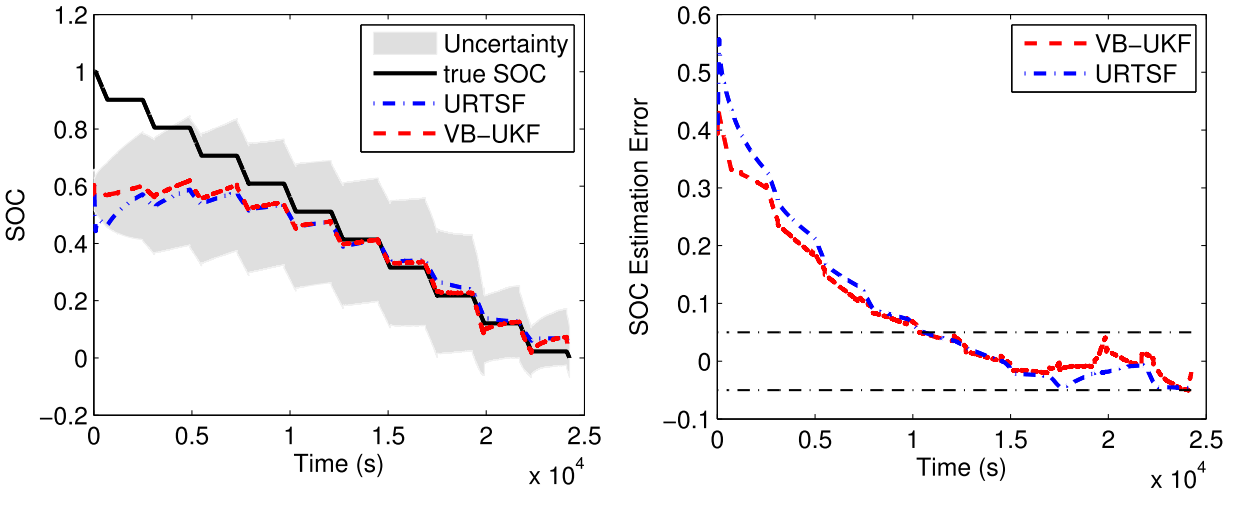

(c) $SOC_0 = 0.6$

FIGURE 8. SOC estimation results in pulsed-discharge test with different initial values (SOC_0).

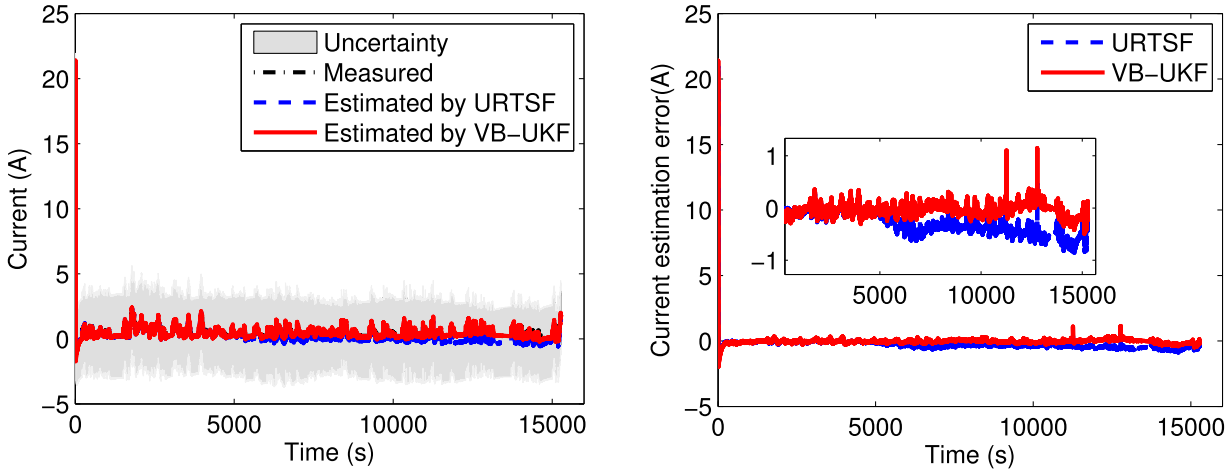

(a) $SOC_0 = 1.0$

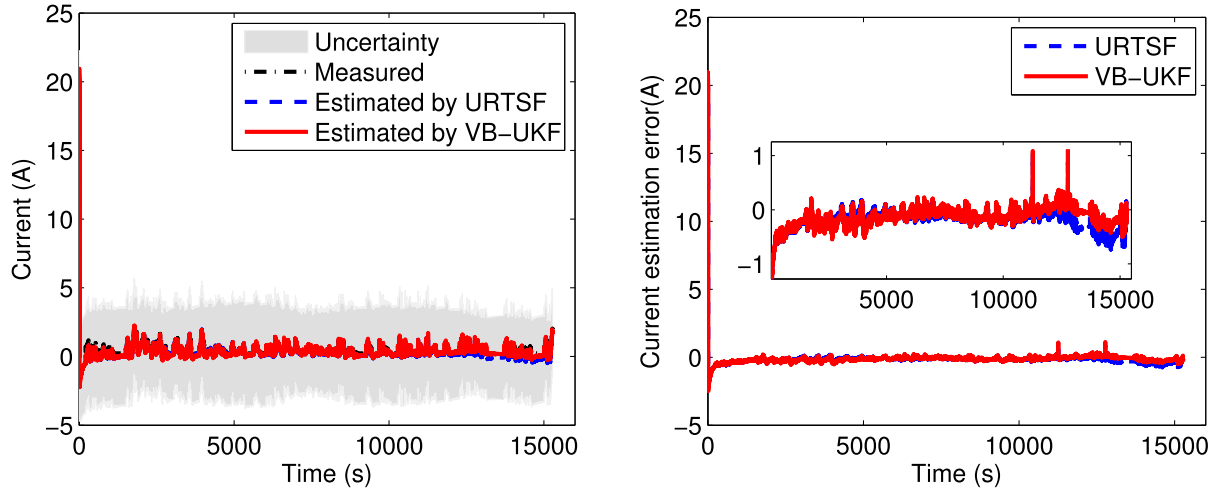

(b) $SOC_0 = 0.8$

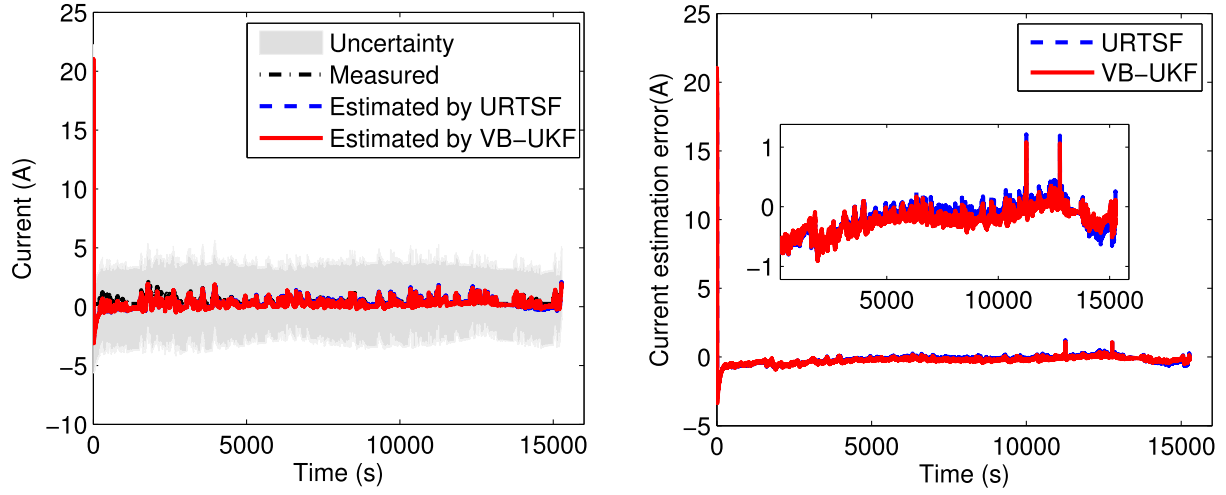

(c) $SOC_0 = 0.6$

FIGURE 9. Current estimation results in UDDS test with different initial values (SOC_0).

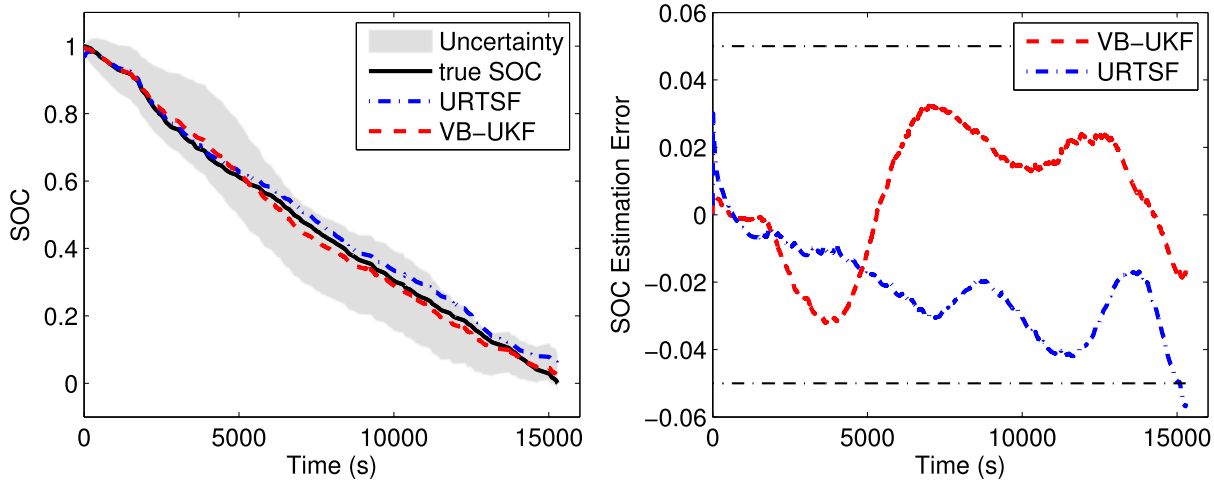

(a) $SOC_0 = 1.0$

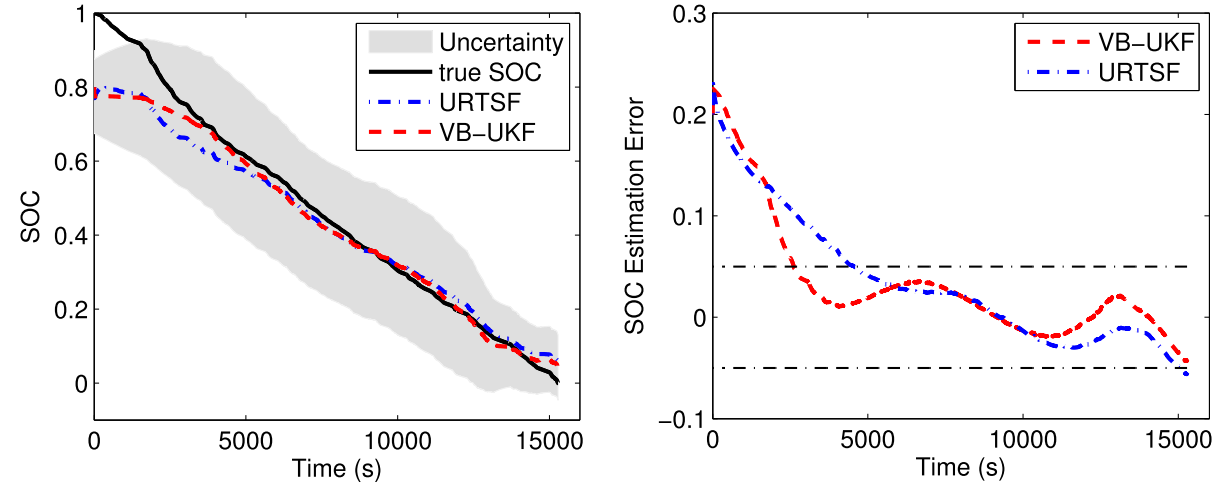

(b) $SOC_0 = 0.8$

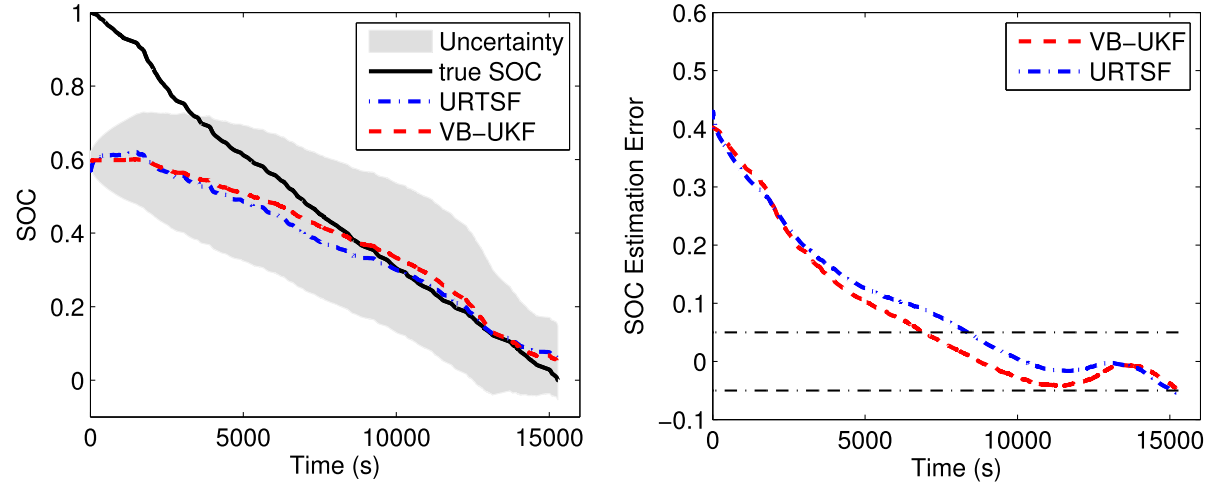

(c) $SOC_0 = 0.6$

FIGURE 10. SOC estimation results in UDDS test with different initial values (SOC_0).

B. EVALUATION IN UDDS TEST

Considering that the pulsed-discharge test is simpler than the load conditions in actual use, a more dynamic operating cycle, UDDS, is employed to verify the SOC estimation performance without current measurement. For initial SOC values 1.0, 0.8 and 0.6, the process noise covariances are $\mathtt{diag}(10^{-6}, 0.1)$, $\mathtt{diag}(10^{-5}, 0.4)$ and $\mathtt{diag}(10^{-5}, 0.1)$, respectively.

The current estimation results are shown in Fig. 9. Apparently, VB-UKF performs better than URTSF in the aspect of estimation accuracy. The MAEs are $0.11A$ and $0.33A$ for VB-UKF and URTSF, respectively, when there is no initial SOC errors. And when $SOC_0 = 0.8$ and $SOC_0 = 0.6$, it can be observed that the current estimation errors do not change with the increase of the SOC estimation errors. It indicates that the current estimations are almost not affected by the SOC estimation results and the initial SOC errors for both URTSF and VB-UKF.

Fig. 10 demonstrates the estimated results of SOC under three initial SOC values. The error analysis and convergence time of these two algorithms are given in Table 3. It is clear that these two algorithms immediately converge to 5% error bound at the correct initial SOC value. Meanwhile, from the angle of MAE and RMSE, we note that the VB-UKF has better SOC estimation accuracy than URTSF. When there are 20% initial SOC error, VB-UKF outperforms URTSF significantly in convergence time and estimation accuracy. As can be seen from Table 3, the convergence time of VB-UKF is about half shorter than URTSF. However, when the initial SOC error increases to 40%, VB-UKF needs 6928s to converge and URTSF needs 8362s to converge, both of the convergence times are much longer than these at $SOC_0 = 80\%$. Meanwhile, it can be seen that the performance superiority of VB-UKF becomes not obvious.

TABLE 3. Error analysis and convergence time with different SOC_0 in UDDS test.

SOC_0	Algorithm	MAE	RMSE	Convergence time (s)
1.0	VB-UKF	1.70%	1.94%	1
	URTSF	2.21%	2.50%	1
0.8	VB-UKF	1.81%	2.13%	2614
	URTSF	2.32%	2.58%	4532
0.6	VB-UKF	2.48%	2.82%	6876
	URTSF	1.83%	2.31%	8355

C. DISCUSSION

From the experimental results in Figs. 7- 10, it is clear that the SOC estimation errors are within the bound of $\pm 5\%$ after convergence for both VB-UKF and URTSF, which is effective and feasible for portable devices without the current sensor. The MAEs of the current estimation are nearby 0.2A, and they are almost not affected by the SOC estimation results. On the contrary, the current estimation accuracy has an influence on the SOC estimation accuracy in the pulsed-discharge test. Larger SOC estimation errors are observed in case of larger current estimation errors when $SOC_0 = 1$.

Meanwhile, we noted that the initial SOC error greatly affects the SOC estimation performance. With correct initial SOC value, both algorithms can obtain fast convergence and good SOC estimation accuracy although the VB-UKF performs slightly better than URTSF. But as the initial SOC error increases, the convergence speed slows down. This phenomenon is more distinct for URTSF. When the initial SOC error is 20%, VB-UKF performs much better than URTSF in convergence speed and SOC estimation accuracy in pulsed-discharge test and UDDS test. These findings indicate that VB-UKF is more accurate and robust than URTSF since its simultaneous estimation of SOC and current, which makes it better compensate the initial SOC error.

However, we also noted that when the initial SOC error continues to increase, VB-UKF has comparable performance with URTSF. Much longer convergence time for VB-UKF is observed. It shows the error correction ability is limited due to the lack of actual current measurement, no matter for VB-UKF or URTSF. However, fortunately, there is usually no such large initial SOC error in portable applications. Moreover, the SOC offset can be gradually calibrated during rest modes.

V. CONCLUSION

Current information is crucial for accurate SOC estimation of the lithium-ion battery. However, the current sensor is often not equipped in portable devices because of the constraints in cost, volume and power. In this study, to estimate the SOC accurately without measuring the current, a novel algorithm of the VB-UKF is proposed. Firstly, by regarding the current as an unknown input, the SOC estimation problem is reformulated as optimal filtering of the nonlinear system with an unknown input. Then, the variational Bayes method is combined with the unscented Kalman filter to simultaneously estimate the SOC and the current input for the nonlinear lithium-ion battery system. Pulsed-discharge test and UDDS test were conducted to validate the SOC estimation performance. Experimental results show that the MAEs and RMSEs of the SOC estimations of the proposed VB-UKF algorithm are less than $\pm 3\%$ after convergence which reveals its feasibility and effectiveness. Moreover, compared to URTSF, VB-UKF exhibits much better SOC estimation performance at small initial SOC errors and comparable performance at large initial SOC errors in terms of accuracy and convergence rate. But, the current estimation accuracy is almost not affected by the initial SOC errors for both VB-UKF and URTSF.

In addition, it is worth noticing that the SOC convergence rate of the proposed algorithm will slow down at large initial SOC errors since there is no current information. But various

measures can be taken to reduce the initial SOC errors such as resting the battery for a period of time, charging the battery full and calibration by the OCV, so this weakness will not affect the usefulness and advancement of the proposed algorithm.

REFERENCES

[1] D. C. Cambron and A. M. Cramer, "A lithium-ion battery current estimation technique using an unknown input observer," *IEEE Trans. Veh. Technol.*, vol. 66, no. 8, pp. 6707–6714, Aug. 2017, doi: 10.1109/TVT.2017.2657520.

[2] H. Dai, G. Zhao, M. Lin, J. Wu, and G. Zheng, "A novel estimation method for the state of health of lithium-ion battery using prior knowledge-based neural network and Markov chain," *IEEE Trans. Ind. Electron.*, vol. 66, no. 10, pp. 7706–7716, Oct. 2019.

[3] K. Liu, C. Zou, K. Li, and T. Wik, "Charging pattern optimization for lithium-ion batteries with an electrothermal-aging model," *IEEE Trans. Ind. Informat.*, vol. 14, no. 12, pp. 5463–5474, Dec. 2018, doi: 10.1109/TII.2018.2866493.

[4] Q. Ouyang, Z. Wang, K. Liu, G. Xu, and Y. Li, "Optimal charging control for lithium-ion battery packs: A distributed average tracking approach," *IEEE Trans. Ind. Informat.*, vol. 16, no. 5, pp. 3430–3438, May 2020, doi: 10.1109/TII.2019.2951060.

[5] S. Wang, S. Yang, W. Yang, and Y. Wang, "A new kind of balancing circuit with multiple equalization modes for serially connected battery pack," *IEEE Trans. Ind. Electron.*, vol. 68, no. 3, pp. 2142–2150, Mar. 2021, doi: 10.1109/TIE.2020.2973886.

[6] R. Xiong, Q. Yu, W. Shen, C. Lin, and F. Sun, "A sensor fault diagnosis method for a lithium-ion battery pack in electric vehicles," *IEEE Trans. Power Electron.*, vol. 34, no. 10, pp. 9709–9718, Oct. 2019, doi: 10.1109/TPEL.2019.2893622.

[7] J. Meng, M. Boukhnifer, C. Delpha, and D. Diallo, "Incipient short-circuit fault diagnosis of lithium-ion batteries," *J. Energy Storage*, vol. 31, Oct. 2020, Art. no. 101658.

[8] J. Li, L. Wang, C. Lyu, and M. Pecht, "State of charge estimation based on a simplified electrochemical model for a single $LiCoO_2$ battery and battery pack," *Energy*, vol. 133, pp. 572–583, Aug. 2017.

[9] X. Feng, C. Xu, X. He, L. Wang, S. Gao, and M. Ouyang, "A graphical model for evaluating the status of series-connected lithium-ion battery pack," *Int. J. Energy Res.*, vol. 43, no. 2, pp. 749–766, Feb. 2019.

[10] X. Lai, Y. Zheng, and T. Sun, "A comparative study of different equivalent circuit models for estimating state-of-charge of lithium-ion batteries," *Electrochim. Acta*, vol. 259, pp. 566–577, Jan. 2018.

[11] X. Zhao, Y. Cai, L. Yang, Z. Deng, and J. Qiang, "State of charge estimation based on a new dual-polarization-resistance model for electric vehicles," *Energy*, vol. 135, pp. 40–52, Sep. 2017.

[12] C. Zhang, K. Li, J. Deng, and S. J. Song, "Improved realtime state-of-charge estimation of $LiFePO_4$ battery based on a novel thermoelectric model," *IEEE Trans. Ind. Electr.*, vol. 64, no. 1, pp. 654–663, Jan. 2017, doi: 10.1109/TIE.2016.2610398.

[13] K. Chwastek, "Modelling hysteresis loops in thick steel sheet with the dynamic Takács model," *Phys. B, Condens. Matter*, vol. 407, no. 17, pp. 3632–3634, Sep. 2012.

[14] X. Hua, C. Zhang, and G. Offer, "Finding a better fit for lithium ion batteries: A simple, novel, load dependent, modified equivalent circuit model and parameterization method," *J. Power Sources*, vol. 484, Feb. 2021, Art. no. 229117.

[15] X. Tang, Y. Wang, C. Zou, K. Yao, Y. Xia, and F. Gao, "A novel framework for lithium-ion battery modeling considering uncertainties of temperature and aging," *Energy Convers. Manage.*, vol. 180, pp. 162–170, Jan. 2019.

[16] H. Dai, T. Xu, L. Zhu, X. Wei, and Z. Sun, "Adaptive model parameter identification for large capacity li-ion batteries on separated time scales," *Appl. Energy*, vol. 184, pp. 119–131, Dec. 2016.

[17] J. Hou, Y. Yang, H. He, and T. Gao, "Adaptive dual extended Kalman filter based on variational Bayesian approximation for joint estimation of lithium-ion battery state of charge and model parameters," *Appl. Sci.*, vol. 9, no. 9, p. 1726, Apr. 2019, doi: 10.3390/app9091726.

[18] Q. Wang, X. Feng, B. Zhang, T. Gao, and Y. Yang, "Power battery state of charge estimation based on extended Kalman filter," *J. Renew. Sustain. Energy*, vol. 11, no. 1, Jan. 2019, Art. no. 014302.

[19] S. Liu, N. Cui, and C. Zhang, "An adaptive square root unscented Kalman filter approach for state of charge estimation of lithium-ion batteries," *Energies*, vol. 10, no. 9, p. 1345, Sep. 2017.

[20] J. Hou, Y. Yang, and T. Gao, "A normal-gamma-based adaptive dual unscented Kalman filter for battery parameters and state-of-charge estimation with heavy-tailed measurement noise," *Int. J. Energy Res.*, vol. 44, no. 5, pp. 3510–3525, Apr. 2020, doi: 10.1002/er.5042.

[21] X. Liu, Z. Chen, C. Zhang, and J. Wu, "A novel temperature-compensated model for power li-ion batteries with dual-particle-filter state of charge estimation," *Appl. Energy*, vol. 123, pp. 263–272, Jun. 2014.

[22] X. Chen, W. Shen, M. Dai, Z. Cao, J. Jin, and A. Kapoor, "Robust adaptive sliding-mode observer using RBF neural network for lithium-ion battery state of charge estimation in electric vehicles," *IEEE Trans. Veh. Technol.*, vol. 65, no. 4, pp. 1936–1947, Apr. 2016, doi: 10.1109/TVT.2015.2427659.

[23] X. Hu, F. Sun, and Y. Zou, "Estimation of state of charge of a lithium-ion battery pack for electric vehicles using an adaptive Luenberger observer," *Energies*, vol. 3, no. 9, pp. 1586–1603, Sep. 2010.

[24] X. Wang, Z. Song, K. Yang, X. Yin, Y. Geng, and J. Wang, "State of charge estimation for lithium-bismuth liquid metal batteries," *Energies*, vol. 12, no. 1, p. 183, Jan. 2019.

[25] M. S. E. Din, M. F. Abdel-Hafez, and A. A. Hussein, "Enhancement in li-ion battery cell state-of-charge estimation under uncertain model statistics," *IEEE Trans. Veh. Technol.*, vol. 65, no. 6, pp. 4608–4618, Jun. 2016.

[26] C. Chen, R. Xiong, and W. Shen, "A lithium-ion battery-in-the-loop approach to test and validate multiscale dual H infinity filters for state-of-charge and capacity estimation," *IEEE Trans. Power Electron.*, vol. 33, no. 1, pp. 332–342, Jan. 2018.

[27] L. Zhao, Z. Liu, and G. Ji, "Lithium-ion battery state of charge estimation with model parameters adaptation using H∞ extended Kalman filter," *Control Eng. Pract.*, vol. 81, pp. 114–128, Dec. 2018.

[28] W. S. Putra, B. R. Dewangga, A. Cahyadi, and O. Wahyunggoro, "Current estimation using thevenin battery model," in *Proc. ICEVT-IMECE*, Surakarta, Indonesia, Nov. 2015, pp. 5–9, doi: 10.1109/ICEVT-TIMECE.2015.7496638.

[29] C. Y. Chun, J. Baek, G.-S. Seo, B. H. Cho, J. Kim, I. K. Chang, and S. Lee, "Current sensor-less state-of-charge estimation algorithm for lithium-ion batteries utilizing filtered terminal voltage," *J. Power Sources*, vol. 273, pp. 255–263, Jan. 2015.

[30] J. Hou, Y. Zhang, T. Gao, and Y. Yang, "Lithium-ion battery state-of-charge estimation without current measurement using unscented recursive three-step filter," in *Proc. 8th Int. Electr. Eng. Congr. (iEECON)*, Chiang Mai, Thailand, Mar. 2020, pp. 1–4, doi: 10.1109/iEECON48109.2020.229495.

[31] M. J. Beal, "Variational algorithms for approximate Bayesian inference," Ph.D. dissertation, Dept. Gatsby Comput. Neurosci. Unit, Univ. College London, U.K., 2003.

[32] S. Sarkka and A. Nummenmaa, "Recursive noise adaptive Kalman filtering by variational Bayesian approximations," *IEEE Trans. Autom. Control*, vol. 54, no. 3, pp. 596–600, Mar. 2009, doi: 10.1109/TAC.2008.2008348.

[33] K. Li, L. Chang, and B. Hu, "A variational Bayesian-based unscented Kalman filter with both adaptivity and robustness," *IEEE Sensors J.*, vol. 16, no. 18, pp. 6966–6976, Sep. 2016, doi: 10.1109/JSEN.2016.2591260.

[34] J. Sun, J. Zhou, and X. R. Li, "State estimation for systems with unknown inputs based on variational Bayes method," in *Proc. 15th Int. Conf. Inf. Fusion*, Singapore, 2012, pp. 983–990.

[35] Q. Wang, J. Kang, Z. Tan, and M. Luo, "An online method to simultaneously identify the parameters and estimate states for lithium ion batteries," *Electrochim. Acta*, vol. 289, pp. 376–388, Nov. 2018.

[36] W. Li and Y. Jia, "State estimation for jump Markov linear systems by variational Bayesian approximation," *IET Control Theory Appl.*, vol. 6, no. 2, pp. 319–326, Jan. 2012, doi: 10.1049/iet-cta.2011.0167.

[37] K. Liu, Y. Li, X. Hu, M. Lucu, and W. D. Widanage, "Gaussian process regression with automatic relevance determination kernel for calendar aging prediction of lithium-ion batteries," *IEEE Trans. Ind. Informat.*, vol. 16, no. 6, pp. 3767–3777, Jun. 2020, doi: 10.1109/TII.2019.2941747.

JING HOU was born in Baoding, Hebei, China, in 1984. She received the B.S. degree in electronic information engineering, the M.S. degree in signal and information processing, and the Ph.D. degree in electronic science and technology from Northwestern Polytechnical University, Xi'an, China, in 2007, 2010, and 2014, respectively.

She is currently an Associate Professor with Northwestern Polytechnical University. Her current research interests include battery state estimation, battery health management and life forecast, and fault diagnosis.

YAN YANG received the B.S. degree in electrical engineering, the M.S. degree in signal and information processing, and the Ph.D. degree in electronic science and technology from Northwestern Polytechnical University, Xi'an, China, in 1992, 2001, and 2008, respectively.

From 1992 to 2001, she was a Research Assistant with the Institute of General Electric, Northwestern Polytechnical University. From 2001 to 2014, she worked as a Lecturer and an Associate Professor with the School of Electronic and Information, Northwestern Polytechnical University, where she has been a Professor, since 2014. Her research interests include modern power conversion technology, power electronics and power drive control, signal detection and estimation, and multisensor information fusion.

TIAN GAO received the B.S. degree in electronic and information engineering from Xi'an Technological University, in 1998, and the M.S. and Ph.D. degrees in electronic science and technology from Northwestern Polytechnical University, in 2005 and 2009, respectively.

He is currently an Associate Professor with Northwestern Polytechnical University. His research interests include battery management and control, wireless power transfer, and power conversion technology.